

Performance of a Monopropellant Thruster Prototype Using Advanced Hydrogen Peroxide Catalytic Beds

L. Torre,^{*} A. Pasini,[†] L. Romeo,[‡] and A. Cervone[§]

ALTA SpA, 56121 Pisa, Italy

and

L. d'Agostino[¶]

University of Pisa, 56126 Pisa, Italy

DOI: 10.2514/1.44354

The present paper illustrates different firing tests carried out on advanced catalytic beds for hydrogen peroxide decomposition in a new monopropellant thruster prototype designed for easier adjustment and control of the main operational and propulsive parameters. The tests refer to the comparison between a Pt/ α -Al₂O₃ catalyst (named FC-LR-87) and a similar commercially available space propulsion catalyst. Up to 2 kg of 87.5% hydrogen peroxide have been decomposed by a single sample of the FC-LR-87 catalyst. Both steady-state and pulsed firings have been carried out in the same reactor configuration. A fresh sample of the FC-LR-87 catalyst has also been tested at a different bed load. Both the FC-LR-87 and the commercial catalysts showed equivalent propulsive performances, with a slight advantage in favor of the FC-LR-87 catalyst in terms of the c^* and temperature efficiencies (up to 94 and 93%, respectively).

Nomenclature

| | |
|--------------|--|
| A | = cross-sectional area, m ² |
| A_t | = throat area, m ² |
| C_F | = thrust coefficient, |
| c^* | = characteristic velocity, m/s |
| D | = catalytic-bed diameter, m |
| D_t | = throat diameter, m |
| F | = thrust, N |
| G | = bed load, kg/m ² s |
| g_o | = sea level gravity acceleration, m/s ² |
| I_{sp} | = specific impulse, s |
| L | = catalytic-bed length, m |
| \dot{m} | = propellant mass flow rate, kg/s |
| p_a | = ambient pressure, Pa |
| p_c | = chamber pressure, Pa |
| R | = gas constant of the exhaust gases, J/mol K |
| T_{ad} | = adiabatic decomposition temperature, K |
| T_{amb} | = ambient temperature, K |
| T_c | = combustion chamber temperature, K |
| T_{exp} | = decomposition temperature (experimentally measured), K |
| α | = conical nozzle half-angle, rad |
| γ | = specific heat ratio of the exhaust gases, |
| η_{c^*} | = characteristic velocity efficiency, |

$\eta_{\Delta T}$ = temperature efficiency,
 τ = dwell time, s

I. Introduction

MONOPROPELLANT propulsion systems are attractive for orbit maintenance and attitude control due to their simplicity, which translates into cost reductions and partially counterbalances their lower specific impulse compared with bipropellant systems. The use of hydrogen peroxide (HP), a nontoxic (or green) monopropellant, offers increased safety and cost-effectiveness in the operation of space propulsion systems, owing to the drastic simplification of the health and safety protection procedures.

High-concentration (or rocket-grade) HP has a long heritage in aerospace propulsion. A wide variety of applications on both manned and unmanned systems can be cited from the 1930s to the present time (Ventura and Garboden [1]). Up to the 1960s a significant amount of work has been carried out by NASA laboratories on HP decomposition and its application to monopropellant rockets (Runckel et al. [2] and Willis [3]). The development of the Shell 405 catalyst and higher-purity hydrazine led to a decreased use of HP due to the superior performance and long-term stability characteristics of hydrazine (Wucherer et al. [4]). In the last decade HP has been receiving a renewed interest for application to cost- and safety-driven systems (Wernimont and Ventura [5] and Scharlemann et al. [6]). Effective operation of HP monopropellant thrusters and gas generators is closely related to the availability of long-lived and reliable catalytic beds, able to provide repetitive performances both in continuous and intermittent operations. The attainment of high decomposition efficiency with reduced bed volumes is a crucial design requirement for HP catalytic reactors in space applications.

A number of different catalyst substrates for HP (including compressed gauzes, pellets, and high-porosity foams [7]) have been employed in the past to achieve these targets. In previous applications, mainly grids, pellets, or beads coated with the catalytic substances have been used, because they maximize the active surface-to-volume ratio. Different metals and metallic oxides deposited on granules or pellets of transition aluminas have been investigated in search for the best catalyst for HP decomposition (Rusek [8], Romeo et al. [9], and Russo Sorge et al. [10]). Furthermore, the influence of stabilizers (such as stannate and pyrophosphate, typically contained in commercial H₂O₂ solutions) on the activity of pellet catalysts has been widely studied (Pirault-Roy et al.

Presented as Paper 4937 at the 44th AIAA/ASME/SAE/ASEE Joint Propulsion Conference, Hartford, CT, 21–23 July 2008; received 13 March 2009; revision received 21 July 2009; accepted for publication 22 July 2009. Copyright © 2009 by the American Institute of Aeronautics and Astronautics, Inc. All rights reserved. Copies of this paper may be made for personal or internal use, on condition that the copier pay the \$10.00 per-copy fee to the Copyright Clearance Center, Inc., 222 Rosewood Drive, Danvers, MA 01923; include the code 0748-4658/09 and \$10.00 in correspondence with the CCC.

^{*}Project Manager, Via Gherardesca 5, Ospedaletto; l.torre@alta-space.com. Member AIAA.

[†]Project Engineer, Via Gherardesca 5, Ospedaletto; Ph.D. Student, Aerospace Engineering Department, University of Pisa; a.pasini@alta-space.com. Member AIAA.

[‡]Project Engineer, Via Gherardesca 5, Ospedaletto; Ph.D. Student, Aerospace Engineering Department, University of Pisa; l.romeo@alta-space.com. Member AIAA.

[§]Project Manager; a.cervone@alta-space.com. Member AIAA.

[¶]Professor, Aerospace Engineering Department; luca.dagostino@ing.unipi.it. Member AIAA.

[11]). The results of screening tests recently carried out on a number of chemical species indicated platinum as the most promising catalyst for HP decomposition [9]. The same tests also indicated that thermal stresses induced by the intense release of heat on the pellet surface often caused the catalyst support to break into fine particles, as commonly observed by a number of investigators (Sahara et al. [12] and Pasini et al. [13]). The efforts to solve this problem recently led to the development of the FC-LR-87 catalyst, a Pt/ α -Al₂O₃ catalyst with a surface load of platinum close to 35% by weight and adequate thermal shock resistance (Romeo et al. [14]). This paper illustrates the results of an experimental campaign carried out by firing the FC-LR-87 and a commercial benchmark catalyst for space propulsion applications in a reconfigurable 5 N monopropellant thruster prototype. The benchmark catalyst (indicated here as Pt/Al₂O₃-COM and produced by a major commercial manufacturer) consists of platinum deposited on the same alumina substrate as a commercial catalyst for hydrazine decomposition. Three different sets of experiments have been conducted to evaluate the propulsive performances of the catalytic beds under consideration:

1) Steady-state firing tests on the FC-LR-87 catalyst were at two different bed loads: 9.92 and 19.26 kg/s \cdot m².

2) Steady-state firing tests on the Pt/Al₂O₃-COM catalyst were at 19.26 kg/s \cdot m² bed load.

3) Pulsed firing tests on the FC-LR-87 catalyst were at 19.26 kg/s \cdot m² bed load.

Scanning electron microscope (SEM) and x-ray diffractometry analyses have also been carried out on the preceding catalysts before and after the firings to assess the possible occurrence of modifications and/or degradations. The results of these analyses are illustrated in a companion paper (Romeo et al. [14]).

II. Test Apparatus

A. Thruster Prototype

Based on the experience gained during previous experimental campaigns (Pasini et al. [13]), a new reconfigurable monopropellant thruster prototype has been designed and realized for investigating different bed configurations under a wide range of operating conditions. The complete decomposition of a given mass flow rate of HP through a catalytic reactor mainly depends on three factors: 1) the characteristics of the catalyst, 2) the dwell time τ of the HP flow, and 3) the operating pressure.

The characteristics of the catalyst determine the activity of the reactor and include the chemical nature of the catalytic substance, the strength of its bond with the carrier, and its dispersion on the support (density of active sites). For a given reactant, the nominal dwell time τ is directly proportional to the bed length L and inversely proportional to bed load G (defined as the reactant mass flow rate divided by the nominal cross section of the catalytic bed). Clearly, longer residence times improve the completion of the decomposition reaction. The chamber pressure affects the reactant concentration and the velocity of the decomposing gas flow in the reactor. Higher operating pressures therefore result in increased decomposition activity and reduced pressure losses through the reactor.

The catalytic bed of the newly designed monopropellant thruster prototype has been realized by means of a modular cartridge for rapid reconfiguration and simplified filling with the catalyst pellets (see Fig. 1). The cartridge consists of a 36-mm-i.d. American Iron and Steel Institute (AISI) 316L stainless steel casing, long enough to accommodate a 100-mm-long catalyst bed between the upstream spring-loaded injection plate and the downstream distribution plate. Two AISI 304 stainless steel screens (37 \times 37 mesh size and 0.2 mm wire diameter) are interposed between the plates and the catalyst for retaining the pellets. Cylindrical inserts with different lengths ($L = 30, 60, \text{ and } 90 \text{ mm}$) and inner diameter ($D = 18 \text{ and } 25 \text{ mm}$) can be inserted inside the cartridge before filling with the catalyst pellets, allowing for easy and independent control of both the dwell time τ and the bed load G . Tight tolerances have been used to prevent HP from channeling along the clearance between the inserts and the casing. In accordance with the indications of the technical literature, the injection and distribution plates have a 50% open-area ratio,

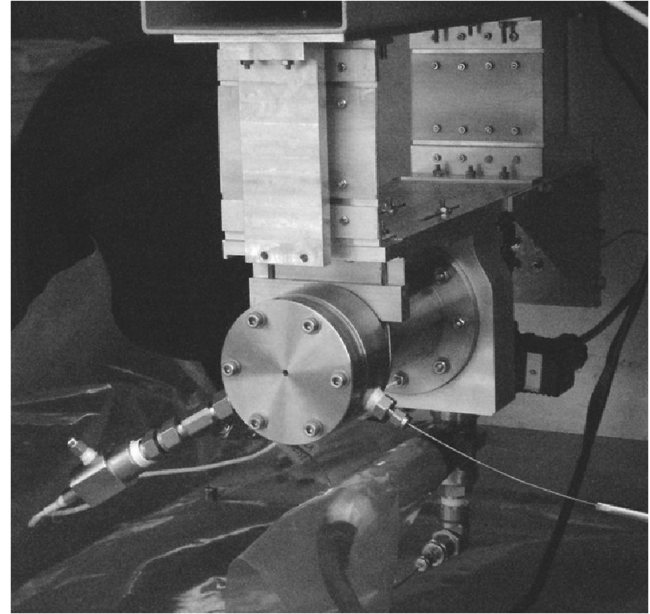


Fig. 1 Photograph of the thruster before a firing test.

realized by means of two different series of holes. The inner part of both plates has a series of eight small holes (1 mm i.d.) for better distributing the flows of HP and decomposition products when using the highest-bed-load configuration, and the outer part has a series of 210 holes (1.5 mm i.d.). A central M3 threaded hole is used for connection to the extracting tool. Once assembled, the cartridge is inserted inside the AISI 316L external housing and directly retained by the HP connecting flange, which seals on two Micatherm S15 face gaskets.

The chamber pressure can easily be adjusted by replacing the separate convergent-divergent nozzle, flanged on the external housing and sealed by a Micatherm S15 face gasket. The thruster prototype has been designed for 5 g/s of 87.5% HP mass flow rate. Using standard isentropic 1-D gas dynamic relations (Cervone et al. [15]), three different conical nozzles have been designed for realizing adapted expansions from 10, 15, and 20 bar (chamber pressure p_c) to 1 atm (ambient pressure p_a). Figure 2 shows the matrix of the accessible test conditions of the catalytic reactor in the present setup in terms of the corresponding values of the operational parameters G and L .

At the current stage of the catalyst development, low values of the bed load have been chosen.

The monopropellant thruster prototype has been designed to be easily interfaced with the thrust balance of the test facility. It is an easily reconfigurable and expandable experimental apparatus

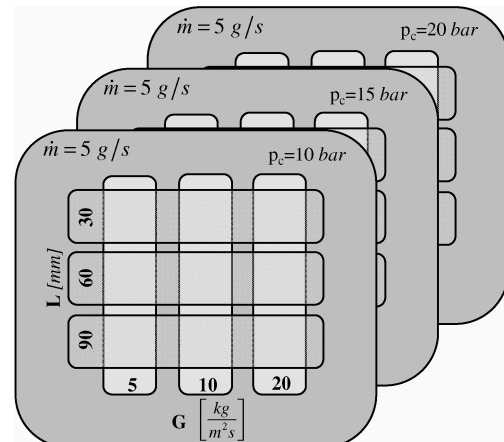


Fig. 2 Matrix of the accessible test conditions of the catalyst reactor in the present setup.

Table 1 Main characteristics of the test thruster

| | | | |
|---------------------------|-------------------------------------|------------|-------------|
| D , mm | 36 | 25 | 18 |
| G , kg/m ² s | 4.91 | 10.19 | 19.65 |
| L , mm | 30/60/90 | 30/60/90 | 30/60/90 |
| τ , s | 8.4/17/25 | 4.1/8.1/12 | 2.1/4.2/6.3 |
| \dot{m} , g/s | 5 | | |
| H_2O_2 | 87.5% (Propulse 875 HTP by Degussa) | | |
| γ | 1.285 | | |
| T_c , K | 952 | | |
| p_c , bar | 10/15/20 | | |
| p_e , atm | 1 | | |
| D_t , mm | 2.40/1.96/1.70 | | |
| A_e/A_t | 2.1/2.7/3.3 | | |
| α , deg | 15 | | |
| F , N | 5.70/6.06/6.28 | | |

especially designed for performance characterization of liquid propellant rocket thrusters (Cervone et al. [15] and Pasini et al. [13]). The main features of the test prototype are summarized in Table 1.

B. Test Data System

The data acquired during a typical firing test are used both for monitoring the operation of the propellant supply system and for evaluating the performance of the thruster prototype. The physical conditions of the propellant stored in the tank are monitored by means of a thermocouple (6-mm-o.d. J-type mineral-insulated thermocouple, produced by Watlow) and a pressure transducer [PTU model produced by Swagelok with a 0–40 bar pressure range and an accuracy of 0.43% full scale output (FSO)]. The HP mass flow rate is regulated by means of a cavitating Venturi for which the differential and outlet pressures are measured, respectively, by a Honeywell FP2000 differential pressure transducer (20–25 bar range, 0.01% FSO accuracy) and a Swagelok PTU pressure transducer (0–40 bar range, 0.43% FSO accuracy). A Coriolis flowmeter (Optimass MFS 7100 S04 produced by Krohne, with a maximum operating pressure of 150 bar, a maximum flow rate of 100 kg/h, and an accuracy of 0.1% of the measured flow rate) has been mounted on the HP feed line for monitoring the propellant mass flux with the required accuracy.

To monitor the performance of the thruster prototype, the following measurements are acquired:

1) Chamber pressure is measured by means of a Kulite pressure transducer model XTM-190M-17 bar, mounted by means of suitable Swagelok connectors on the external housing of the thruster.

2) Pressure drop across the catalytic bed is measured by means of a FP2000 differential pressure transducer produced by Honeywell (500 psi range, 0.1% FSO accuracy).

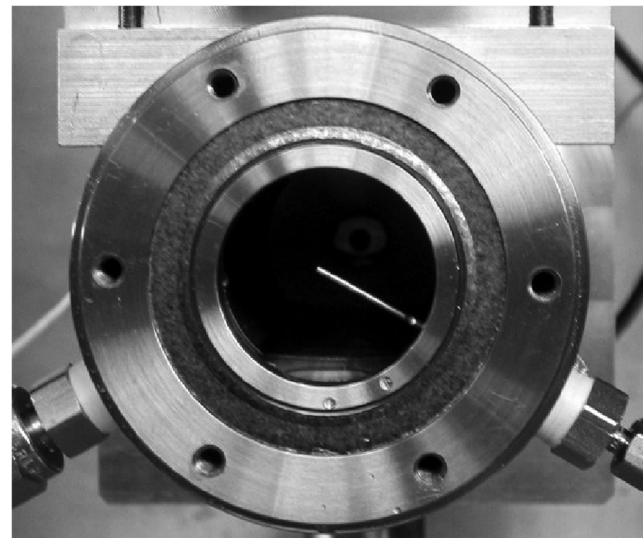


Fig. 3 Axial photograph of the thrust chamber (without the nozzle), showing the location of the thermocouple.

3) Chamber temperature is measured by means of a 1-mm-diam K-type mineral-insulated thermocouple mounted on the catalytic reactor housing by means of an adjustable 1/8 in. National Pipe Thread threaded bushing, with the sensing tip located on the chamber axis (see Fig. 3).

4) Thrust is measured by means of a subminiature compression load cell (Sensotec model 13) with 1 kgf full scale and a maximum combined error (nonlinearity, hysteresis, and repeatability) of 0.9% FSO.

A dc source, capable of supplying different output voltages, provides the transducers with the required electric excitations. The data coming from the sensors and transducers installed in the facility are acquired and transferred to a personal computer by means of a National Instruments acquisition board, capable of acquiring 32 analogical and 48 digital channels at a maximum sample rate of 1.25 megasamples/second. The acquisition board is connected to different signal conditioning extension for instrumentation conditioning and filtering modules produced by National Instruments. A LabVIEW® data acquisition and control program performs real-time display of the data and records all of the acquired signals. A 20-samples/second acquisition rate has been selected for compatibility with the maximum speed of the acquisition board and the CPU, which represents the real limitation of the actual configuration. Pressure, mass flow rate, and thrust and temperature signals have been low-pass-filtered, respectively, by means of a 10 and 4 Hz cutoff-frequency analog Butterworth filter. Figure 4 shows a schematic of the arrangement of the transducers and thermocouples used.

III. Catalysts

As a result of the preliminary assessment of different platinum-based catalysts (Romeo et al. [16]), a Pt/ α -Al₂O₃ catalyst, named FC-LR-87, has been selected for testing in the thruster prototype, owing to its excellent chemical activity and adequate thermal shock resistance. A platinum catalyst (indicated here as Pt/Al₂O₃-COM), produced by W. C. Heraeus, GmbH, and supported on alumina granules with monodispersed diameters ranging from 0.71 to 0.85 mm, has also been procured to compare the FC-LR-87 propulsive performances with those of a typical commercial benchmark for space propulsion applications (see Fig. 5). The Pt/Al₂O₃-COM catalyst employs the same substrate used for the H-KC-12-GA catalyst for hydrazine decomposition previously produced by Solvay. The catalyst carrier, obtained by means of a suitable sol-gel procedure capable of yielding nearly spherical granules for more uniform bed packing and reduced pressure drop [17], has a consistent record of long duration. In fact, up to 300,000 firing pulses have been carried out in a 20, 4, and 1 N hydrazine monopropellant thruster [18] using the same substrate as the Pt/Al₂O₃-COM catalyst with a different active species. The choice of this catalyst support has been motivated by the fact that similar thermomechanical conditions are expected in the present HP decomposition tests in the thruster prototype.

- (T) thermocouple
- (P) pressure transducer
- (LC) load cell
- (ΔP) differential pressure transducer

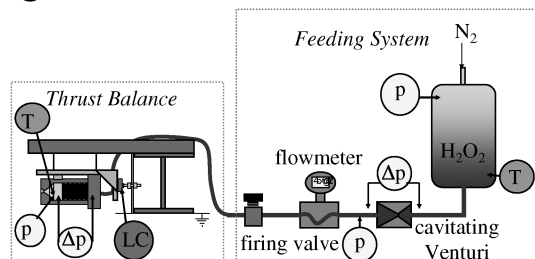


Fig. 4 Schematic of the thrust balance and the HP feed system, showing the transducer arrangement and location.

Table 2 Main characteristics of the catalytic systems used in the thruster experimental campaign

| | FC-LR-87 | Pt/Al ₂ O ₃ -COM |
|---------------------------|---|---|
| Catalyst | Pt/α-Al ₂ O ₃ α-alumina spheres produced by SASOL, GmbH Diameter: 0.6 mm, Brunauer–Emmett–Teller surface area: 4 m ² /g | Pt/Al ₂ O ₃ Alumina grains produced by W. C. Heraeus, GmbH Grain size: 0.71–0.85 mm |
| Support | Brunauer–Emmett–Teller | |
| Nominal metal load (wt %) | 2 | 10 |
| SEM metal load (wt %) | 35 | 8 |

The main properties of the catalysts under investigation are reported in Table 2. The nominal platinum load of the Pt/Al₂O₃-COM catalyst is 10% by weight. The last column in Table 2 reports the average platinum load, expressed in atomic weight percent (wt %), obtained from several SEM readings using a standard crossover window (240 × 200 μm). The full SEM spectra are presented in a companion paper (Romeo et al. [14]).

IV. Experimental Results and Discussion

The FC-LR-87 catalyst has been tested in steady-state operation at two different values of the bed load and in pulsed operation at the highest bed load. The results have been compared with those obtained for the Pt/Al₂O₃-COM catalyst under steady-state conditions

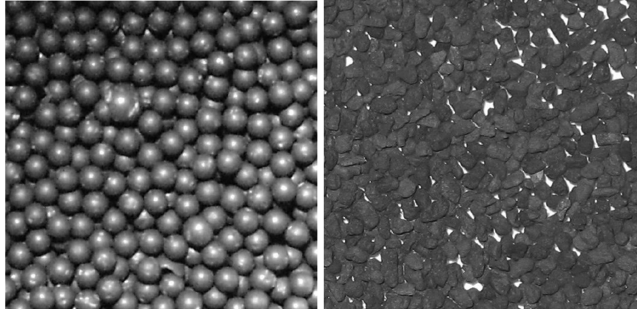


Fig. 5 FC-LR-87 catalyst (left) and the Pt/Al₂O₃-COM catalyst (right).

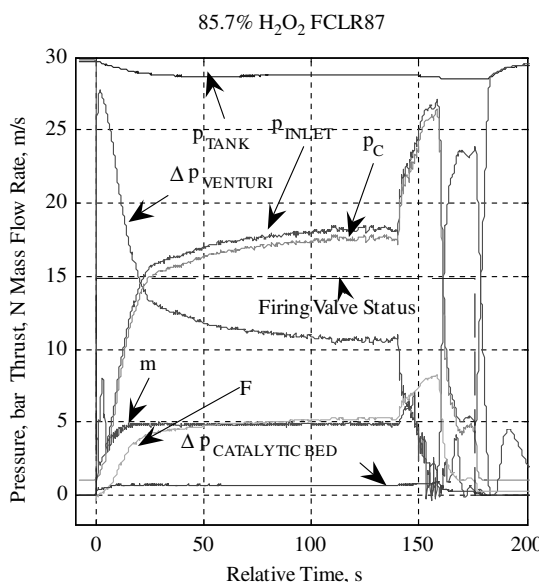


Fig. 6 Experimental results for the FC-LR-87 catalyst tested with 85.7% HP at $G = 19.02 \text{ kg/s m}^2$ and $\tau = 4.34 \text{ s}$.

at the highest bed load. Before each experiment, the actual concentration of the hydrogen peroxide solution has been measured by means of an Abbé refractometer.

A. Catalytic-Bed Main Parameters and Propulsive Performance

The capability of a catalytic bed of effectively decomposing HP to generate thrust can be assessed by means of the characteristic velocity efficiency (c^* efficiency) and the temperature efficiency. In the c^* efficiency, the experimental characteristic velocity (computed from the measurements of the propellant mass flow rate, the chamber pressure, and the nozzle throat cross-sectional area) is compared with the theoretical characteristic velocity corresponding to the ideal case of complete adiabatic decomposition:

$$\eta_{c^*} = \frac{c_{\text{exp}}^*}{c_{\text{theo}}^*} = \frac{p_c^{\text{exp}} A_t}{\dot{m}_{\text{exp}}} / \left[\sqrt{\frac{RT_{\text{ad}}}{\gamma}} \left(\frac{\gamma + 1}{2} \right)^{\frac{\gamma+1}{\gamma-1}} \right] \quad (1)$$

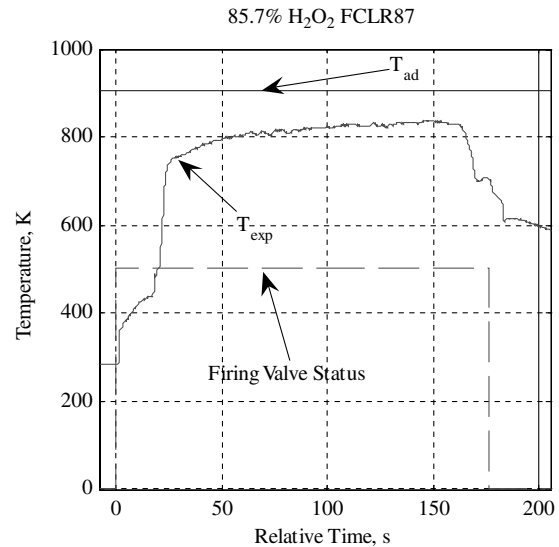


Fig. 7 Chamber temperature for the FC-LR-87 catalyst tested with 85.7% HP at $G = 19.02 \text{ kg/s m}^2$ and $\tau = 4.34 \text{ s}$.

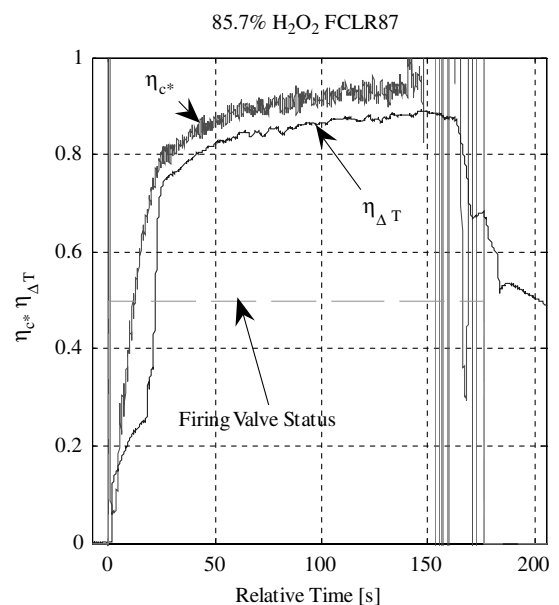


Fig. 8 Temperature and c^* efficiencies for the FC-LR-87 catalyst tested with 85.7% HP at $G = 19.02 \text{ kg/s m}^2$ and $\tau = 4.34 \text{ s}$.

Table 3 Steady-state performance parameters of the FC-LR-87 catalyst tested with 85.7% HP at $G = 19.02 \text{ kg/s m}^2$ and $\tau = 4.34 \text{ s}$

| Performance | FC-LR-87 | Ideal adiabatic decomposition |
|--|----------|-------------------------------|
| Bed load, $\text{kg/s} \cdot \text{m}^2$ | 19.02 | — |
| Dwell time, s | 4.34 | — |
| Mass flow rate, g/s | 4.84 | 4.84 |
| Chamber pressure, bar | 17.5 | 18.7 |
| Chamber temperature, K | 831 | 906 |
| Characteristic velocity, m/s | 822 | 883 |
| Thrust, N | 5.2 | 5.9 |
| Thrust coefficient | 1.31 | 1.38 |
| Specific impulse, s | 110 | 124 |
| Vacuum specific impulse, s | 145 | 164 |
| Catalytic-bed pressure drop, bar | 0.65 | — |
| c^* efficiency | 0.94 | — |
| ΔT efficiency | 0.88 | — |

The discrepancy between experimental and theoretical characteristic velocity is due to the actual decomposition temperature (which is lower than the adiabatic decomposition temperature) and to the non-idealities of the real expansion in the thrust chamber (the assumptions of the quasi-1-D theory of ideal rockets are not accurately satisfied). The temperature efficiency just highlights the first cause of degradation of the characteristic velocity, expressing how close the measured chamber temperature is to the adiabatic temperature corresponding to complete decomposition of the propellant:

$$\eta_{\Delta T} = \frac{T_{\exp} - T_{\text{amb}}}{T_{\text{ad}} - T_{\text{amb}}} \quad (2)$$

In propulsive applications, another important operational parameter is the pressure drop across the catalytic bed. It obviously affects the propellant pressurization system and it usually should be minimized to reduce the overall mass of the propellant feed system. Its theoretical evaluation is quite uncertain because of its complex dependence on several operating parameters (bed porosity, pellet shape and size, bed length and load, and the pressure, temperature, density, and velocity of the bed flow), most of which are only imperfectly known.

Finally, the thrust balance allows for the measurement of the thrust history and therefore of the experimental thrust coefficient:

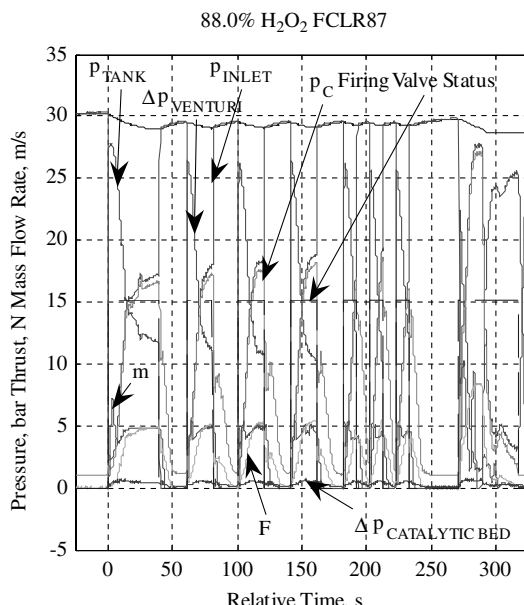


Fig. 9 Experimental results for the FC-LR-87 catalyst with 88.0% HP at $G = 19.02 \text{ kg/s m}^2$ and $\tau = 4.34 \text{ s}$.

$$C_F^{\exp} = \frac{F_{\exp}}{p_c^{\exp} A_t} \quad (3)$$

Together with the experimental characteristic velocity, the thrust coefficient allows for the evaluation of the specific impulse,

$$I_{\text{sp}}^{\exp} = \frac{c_{\exp}^* C_F^{\exp}}{g_0} \quad (4)$$

the thruster's most relevant operational parameter for propulsive purposes.

For each test, the measured histories of the pressure, temperature, thrust, and propellant mass flow rate of the thruster are reported in the next sections, together with the computed histories of the c^* and temperature efficiencies.

B. Steady-State Test of the FC-LR-87 Catalyst with 85.7% HP at $G = 19.02 \text{ kg/s m}^2$ and $\tau = 4.34 \text{ s}$

To evaluate the steady-state performance of the FC-LR-87 catalyst, 850 g of 85.7% HP have been decomposed in a single 150-s-long firing. Figures 6 and 7 report the measured experimental data. The firing valve has been closed after complete depletion of the propellant tank (relative time is 175 s), but the mass flow rate has been controlled only up to a relative time of 140 s, when the last drop of liquid HP passed through the throat of the cavitating Venturi. After an initial transient phase lasting about 25 s, the thruster essentially reached steady-state operation for about 115 s. The thrust history was particularly smooth and there were no appreciable pressure oscillations in the thrust chamber. The pressure drop across the catalytic bed was quite low and the chamber temperature reached 831 K.

Figure 7 shows that the relatively long initial transient is due to the time needed for evaporating the HP/water mixture at the local pressure level. Once evaporation is completed, the slope of the temperature curve rapidly increases. The time evolution of the efficiencies is reported in Fig. 8. In steady-state operation, the temperature and c^* efficiencies reaches about 88 and 94%, respectively.

The main steady-state performance parameters of the FC-LR-87 catalyst are summarized in Table 3. The relatively low value of the bed load (19.02 kg/s m^2) resulted in a low pressure drop across the catalytic bed and a high degree of HP decomposition at steady-state conditions, but is probably also responsible for the long initial transient due to the delayed pressurization of the catalytic bed and the

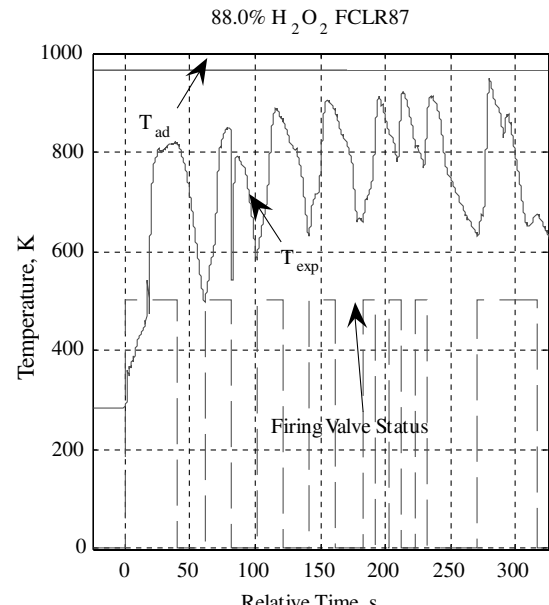


Fig. 10 Chamber temperature for the FC-LR-87 catalyst with 88.0% HP at $G = 19.02 \text{ kg/s m}^2$ and $\tau = 4.34 \text{ s}$.

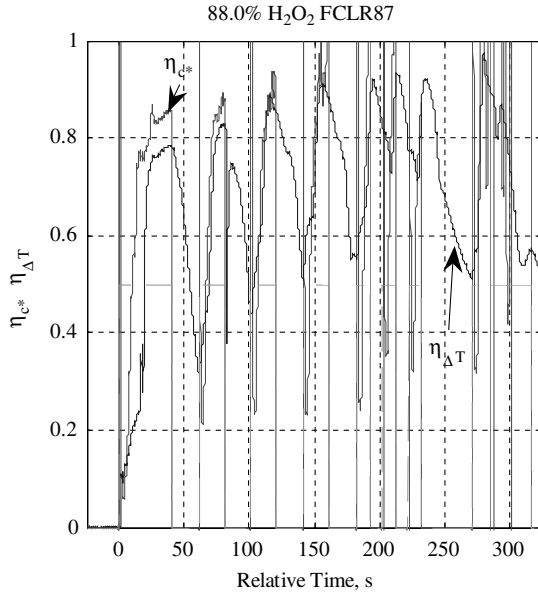


Fig. 11 Temperature and c^* efficiencies for the FC-LR-87 catalyst with 88.0% HP at $G = 19.02 \text{ kg/s m}^2$ and $\tau = 4.34 \text{ s}$.

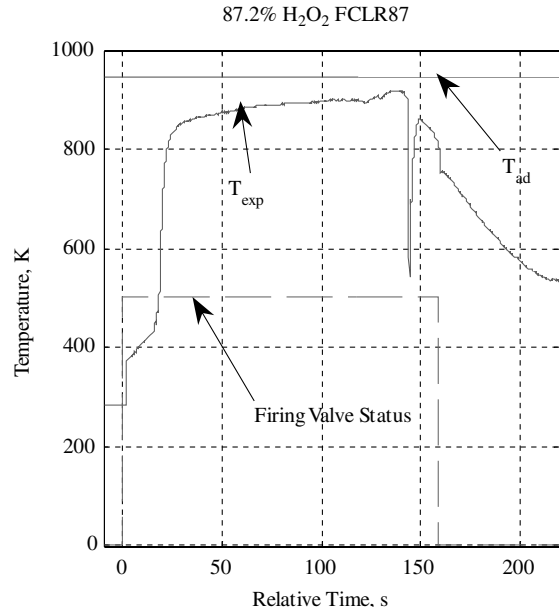


Fig. 13 Chamber temperature for the FC-LR-87 catalyst tested with 87.2% HP at $G = 9.92 \text{ kg/s m}^2$ and $\tau = 8.32 \text{ s}$.

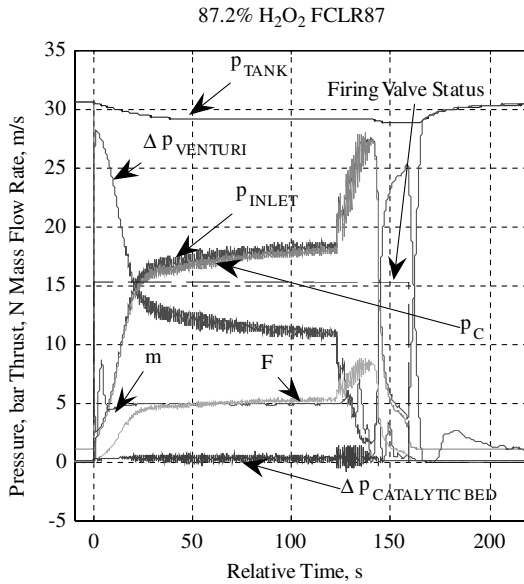


Fig. 12 Experimental results for the FC-LR-87 catalyst tested with 87.2% HP at $G = 9.92 \text{ kg/s m}^2$ and $\tau = 8.32 \text{ s}$.

consequent reduced chemical activity and heat transfer to the catalyst pellets. The vacuum specific impulse reported in Table 3 has been computed with the assumption of ideal expansion to Mach 5.

C. Pulsed Test of the FC-LR-87 Catalyst with 88.0 % HP at $G = 19.02 \text{ kg/s m}^2$ and $\tau = 4.34 \text{ s}$

The same catalytic bed used in steady-state conditions has also been tested in intermittent pulsed operation. The duty cycle consisted of a 40 s firing followed by a 20 s pause, a first series of three 20 s firings separated by 20 s pauses, and a final series of three 10 s pulses separated by 10 s pauses (see Fig. 9). Because the initial transient turned out to be almost coincident with that of the steady-state testing, the catalytic-bed activity did not show any degradation and demonstrated good repeatability.

As a consequence of the heating of the catalytic bed during the first 40 s firing, in later pulses, the initial temperature of the catalytic bed was higher than the evaporation threshold (about 500 K) and duration of the startup transient was almost halved (see Fig. 10).

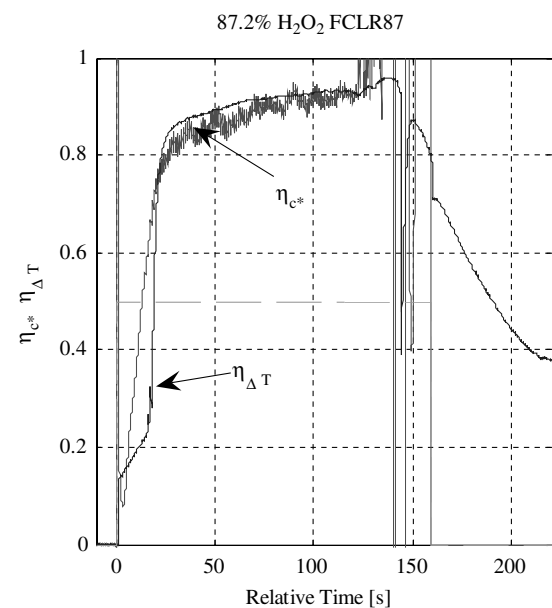


Fig. 14 Temperature and c^* efficiencies for the FC-LR-87 catalyst tested with 87.2% HP at $G = 9.92 \text{ kg/s m}^2$ and $\tau = 8.32 \text{ s}$.

In the last series of three pulses, the temperature efficiency exceeded 90%, a value higher than in the first firing (see Fig. 11). In this case, the evaluation of the c^* efficiency is not particularly meaningful because steady-state conditions were never achieved. However, the transient trend of the time evolution of the c^* efficiency is similar to the one displayed in the first pulsed firing.

D. Steady-State Test of the FC-LR-87 Catalyst with 87.2% HP at $G = 9.92 \text{ kg/s m}^2$ and $\tau = 8.32 \text{ s}$

To investigate potential improvements of HP decomposition the FC-LR-87 catalyst has also been tested at lower value of the bed load ($G = 9.92 \text{ kg/s m}^2$) in a larger catalytic bed according to the same experimental procedure used in the previous steady-state firing. Figure 12 and 13 report the measured data of the test. Also in this case, the firing valve has been closed only after the complete depletion of the HP tank. The reduced value of the bed load allowed

Table 4 Steady-state performance of the FC-LR-87 catalyst tested with 87.2% HP at $G = 9.92 \text{ kg/s m}^2$ and $\tau = 8.32 \text{ s}$

| Performance | FC-LR-87 | Ideal adiabatic decomposition |
|--|----------|-------------------------------|
| Bed load, $\text{kg/s} \cdot \text{m}^2$ | 9.92 | — |
| Dwell time, s | 8.32 | — |
| Mass flow rate, g/s | 4.87 | 4.87 |
| Chamber pressure, bar | 18.0 | 19.5 |
| Chamber temperature, K | 900 | 945 |
| Characteristic velocity, m/s | 840 | 900.5 |
| Thrust, N | 5.3 | 6.1 |
| Thrust coefficient | 1.31 | 1.38 |
| Specific impulse, s | 110 | 127 |
| Vacuum specific impulse, s | 145 | 167 |
| Catalytic-bed pressure drop, bar | 0.30 | — |
| c^* efficiency | 0.93 | — |
| ΔT efficiency | 0.93 | — |

for the decrease of the pressure drop across the catalytic bed and the improvement of the temperature efficiency (Fig. 14) from 88 to about 93%.

The main steady-state performance parameters are reported in Table 4. The chamber temperature was slightly higher than that of the first firing because of the different concentration of the HP solution (87.2% instead of 85.7%). In the steady-state phase, pressure oscillations were detected inside the chamber. The origin of these oscillations has not been investigated, but the very low value of the pressure losses in the reactor bed clearly did not effectively contribute to damp them out. Finally, the peak in the temperature efficiency in the last part of the firing, when the cavitating Venturi is no longer able to stabilize the mass flow rate, is an artifact due to the unsteady increase of the chamber pressure and mass flow rate during the final depletion transient of the catalytic bed.

E. Steady-State Test of the Pt/Al₂O₃-COM Catalyst with 87.7% HP at $G = 19.26 \text{ kg/s m}^2$ and $\tau = 4.28 \text{ s}$

Figures 15 and 16 show the time evolution of the measured experimental data for the steady-state firing of the Pt/Al₂O₃-COM catalyst during the decomposition of more than 1 kg of 87.7% HP. After the initial transient of about 50 s, when the chamber pressure approached a steady value of about 17 bar, a second transient seems to have occurred with a new asymptotic value of the chamber pressure close to 20 bar. This finding was particularly unexpected

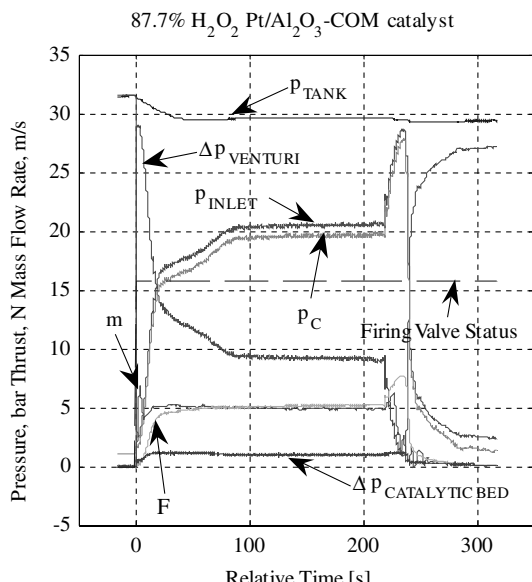


Fig. 15 Experimental results for the Pt/Al₂O₃-COM catalyst tested with 87.7% HP at $G = 19.26 \text{ kg/s m}^2$ and $\tau = 4.28 \text{ s}$.

because it was not associated with any significant changes of the HP mass flow rate, the thrust, and the chamber gas temperature.

The reason for this behavior became manifest during the examination of the thruster after the firing. Figure 17 shows a photograph of the converging part of the stainless steel nozzle, which displayed clear signs of chemical attack by the flow of HP decomposition products. Chemical analysis showed that this phenomenon was due to the high content of chlorides on the surface of the catalyst, for which the release of chlorine deteriorated the passivated layer of the stainless steel nozzle, allowing the hydrous ferrous oxides to rust the throat. As a consequence, the overall dimensions of the throat

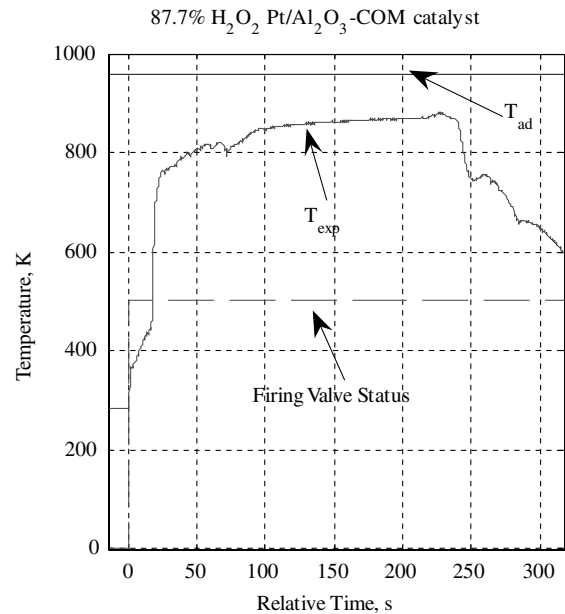


Fig. 16 Chamber temperature for the Pt/Al₂O₃-COM catalyst tested with 87.7% HP at $G = 19.26 \text{ kg/s m}^2$ and $\tau = 4.28 \text{ s}$.

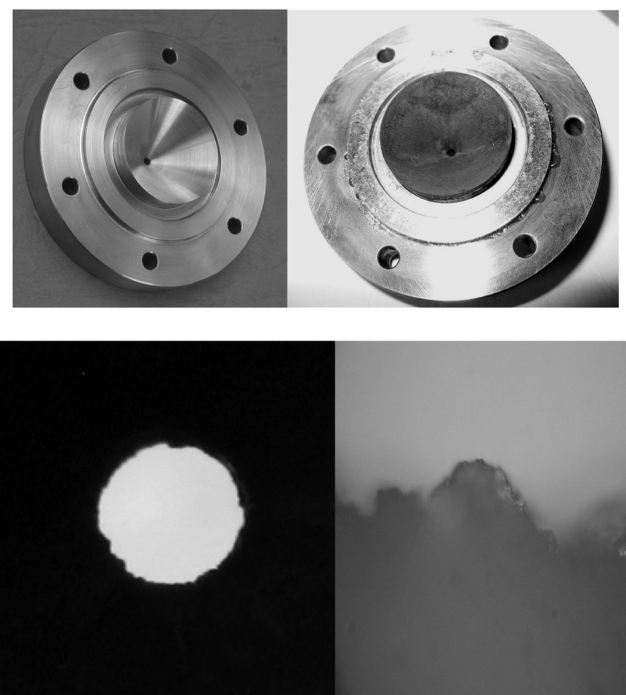


Fig. 17 Nozzle (top) before and after the firing performed with Pt/Al₂O₃-COM catalyst and the partially obstructed throat section (bottom).

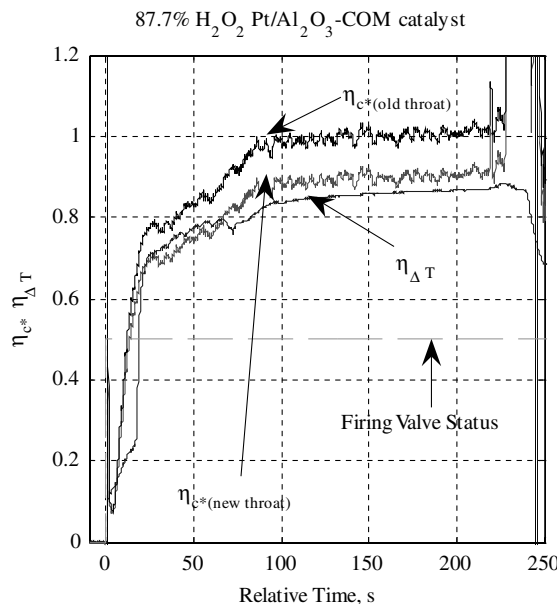


Fig. 18 Temperature and c^* efficiencies of the $\text{Pt}/\text{Al}_2\text{O}_3$ -COM catalyst tested with 87.7% HP at $G = 19.26 \text{ kg/s} \cdot \text{m}^2$ and $\tau = 4.28 \text{ s}$.

changed during the firing, decreasing from 1.70 to about 1.61 mm (Fig. 17, on the right). This explains the reduction of the thrust coefficient with respect to previous firings and the parallel increase of the chamber pressure.

The throat diameter change is also evident in the time evolution of the c^* efficiency (see Fig. 18). Using the nominal dimension of the throat, after the initial 50-s-long transient, the c^* efficiency reached values incompatible with the actual value of the temperature efficiency. On the other hand, when the new steady-state condition was reached (from a relative time of 100 s until the end of the firing), the c^* efficiency computed from the new value of the throat measured in the postfiring examination was fully consistent with the test results.

Table 5 summarizes the steady-state performance parameters of the thruster operating with the $\text{Pt}/\text{Al}_2\text{O}_3$ -COM catalyst. It is evident that the peak values of the chamber pressure, the temperature, and c^* efficiencies are slightly lower than the corresponding values obtained using FC-LR-87 in the same catalytic-bed configuration and operational condition. Also in the case of the $\text{Pt}/\text{Al}_2\text{O}_3$ -COM catalyst, the thrust history is particularly smooth and there is no evidence of pressure oscillations in the thrust chamber. The pressure drop across the catalytic bed (1 bar), although still rather low, is slightly higher than for the FC-LR-87 catalyst under the same working conditions, most likely as a consequence of the more irregular shape of the substrate pellets.

Table 5 Steady-state performance parameters of the $\text{Pt}/\text{Al}_2\text{O}_3$ -COM catalyst tested with 87.7% H_2O_2 at $G = 19.26 \text{ kg/s m}^2$ and $\tau = 4.28 \text{ s}$

| Performance | $\text{Pt}/\text{Al}_2\text{O}_3$ -COM | Ideal adiabatic decomposition |
|--|--|-------------------------------|
| Bed load, $\text{kg/s} \cdot \text{m}^2$ | 19.26 | — |
| Dwell time, s | 4.28 | — |
| Mass flow rate, g/s | 4.90 | 4.90 |
| Chamber pressure, bar | 19.6 | 21.5 |
| Chamber temperature, K | 870 | 958 |
| Characteristic velocity, m/s | 840 | 900.5 |
| Thrust, N | 5.2 | 6.2 |
| Thrust coefficient | 1.30 | 1.40 |
| Specific impulse, s | 110 | 130 |
| Vacuum specific impulse, s | 142 | 168 |
| Catalytic-bed pressure drop, bar | 1.0 | — |
| c^* efficiency | 0.90 | — |
| ΔT efficiency | 0.865 | — |

V. Conclusions

In present tests on the thruster prototype, the $\text{Pt}/\alpha\text{-Al}_2\text{O}_3$ catalytic bed has shown good and constant propulsive performance. At the present stage of development of HP catalysts for rocket thruster applications, the following main conclusions can be drawn:

1) The thermomechanical resistance of the $\alpha\text{-Al}_2\text{O}_3$ substrate seems to be compatible with typical rocket thruster applications without danger of rupture and powdering of the ceramic pellets.

2) The novel catalyst deposition technique on the alumina pellets has succeeded in realizing high surface loads of platinum on the $\alpha\text{-Al}_2\text{O}_3$ substrate in spite of its relative low surface area ($4 \text{ m}^2/\text{g}$).

3) High decomposition efficiencies have been obtained with a platinum-deposited surface of the same order of magnitude of the geometrical surface area of the substrate pellets.

The new monopropellant thruster prototype has allowed for the investigation of different bed configurations and demonstrated the capability of easily adjusting the operating parameters over their design range of variation. On the other side, the need of a more flexible and reconfigurable prototype has led to a final design that is not optimized for reducing the weight.

Despite the long initial transient caused by the low values of the bed load and the high thermal inertia of the system, the steady-state propulsive performance of the thruster has been satisfactory. In particular, both the temperature and c^* efficiencies exceeded the value of 90%. Furthermore, the catalytic-bed activity has not shown any degradation and has demonstrated a good repeatability even after the decomposition of about 2 kg of high-grade HP.

Moreover, the comparison between FC-LR-87 catalyst and the commercial benchmark showed that both catalysts attained similar propulsive performances, and the FC-LR-87 catalyst actually proved to be slightly superior in terms of c^* and temperature efficiencies and pressure losses. Finally, the high contents of chlorides on the surface of the $\text{Pt}/\text{Al}_2\text{O}_3$ -COM catalyst make it incompatible with the use of stainless steel for realizing the thruster, whereas the FC-LR-87 catalyst does not suffer from this limitation. Furthermore, both catalysts have shown the same transient behavior, suggesting that the observed performance during the pulsed tests is mainly connected with the choice of the operational parameters (bed load, bed length, initial preheating, etc.) and not with the intrinsic HP decomposition capabilities of these catalysts.

To improve the decomposition activity of the catalytic bed, catalyst development will be focused on the impregnation of smaller pellets for increasing the overall active surface of the catalyst under the same catalytic-bed arrangement. The pressure-loss penalty associated with the reduction of the typical dimension of the spheres seems to not be a real problem, because the pressure drops experienced in the tests reported in this paper are very low and far from unaffordable values. As a matter of fact, the decomposition rate and the transient response could actually take advantage of the more rapid increase of the pressure in the catalytic bed caused by higher pressure losses. Furthermore, the increase of the active area associated with the reduction of the pellets size is expected to provide margins for the decreasing of the overall dimensions of the catalytic bed down to realistic values for rocket thruster applications.

The influence of the operational parameters on the transient startup must be investigated to reduce the initial transient phase. Because most of the transient is due to the time needed for completing the evaporation of the HP propellant, the increase of the bed pressure and possibly the use of a preheater seem to be the most viable solutions.

Acknowledgments

The authors gratefully acknowledge the support of the Italian Ministry for Production Activities under Decreto Ministeriale 593. The authors would like to express their gratitude to Mariano Andrenucci, Fabrizio Paganucci, and Renzo Lazzaretti of the Dipartimento di Ingegneria Aerospaziale, Università di Pisa, for their constant and friendly encouragement and to Paolo Moretti, Alberto Grechi, and the other students who contributed to the project. Special thanks go to Massimo d'Urso, who manufactured the monopropellant prototype with great passion.

References

- [1] Ventura, M., and Garboden, G., "A Brief History of Concentrated Hydrogen Peroxide Uses," 35th AIAA/ASME/SAE/ASEE Joint Propulsion Conference, AIAA Paper 99-2739, Los Angeles, June 1999.
- [2] Runckel, J. F., Willis, C. M., Salters, L. B., Jr., "Investigation of Catalyst Beds for 98-Percent-Concentration Hydrogen Peroxide," NASA Langley Research Center, TN D-1808, Hampton, VA, 1963.
- [3] Willis, C. M., "The Effect of Catalyst-Bed Arrangement on Thrust Buildup and Decay Time for a 90 Percent Hydrogen Peroxide Control Rocket," NASA TN D-516, 1960.
- [4] Wucherer, E. J., Cook, T., Stiefel, M., Humphries, R., Parker, J., "Hydrazine Catalyst Production-Sustaining S-405 Technology," 39th AIAA/ASME/SAE/ASEE Joint Propulsion Conference, AIAA Paper 03-5079, Huntsville, AL, July 2003.
- [5] Wernimont, E., and Ventura, M., "Low Temperature Start & Operation Capability of 82% Hydrogen Peroxide Gas Generators," 5th International Spacecraft Propulsion Conference and 2nd International Symposium on Propulsion for Space Transportation, Heraklion, Crete, Greece, May 2008.
- [6] Scharlemann, C., Schiebl, M., Marhold, K., Tajmar, M., Miotti, P., Kappenstein, C., Batonneau, Y., Brahmi, R., and Hunter, C., "Development and Test of a Miniature Hydrogen Peroxide Monopropellant Thruster," 42nd AIAA/ASME/SAE/ASEE Joint Propulsion Conference and Exhibit, AIAA 06-4550, Sacramento, CA, July 2006.
- [7] Barley, S., Palmer, P., Wallbank, J., and Baker, A., "Characterization of a Monopropellant Microthruster Catalytic Bed," 41st Joint Propulsion Conference, AIAA Paper 05-4544, Tucson, AZ, 2005.
- [8] Rusek, J., "New Decomposition Catalysts and Characterization Techniques for Rocket-Grade Hydrogen Peroxide," *Journal of Propulsion and Power*, Vol. 12, No. 3, 1996, p. 574.
doi:10.2514/3.24071
- [9] Romeo, L., Torre, L., Pasini, A., Cervone, A., d'Agostino, L., and Calderazzo, F., "Performance of Different Catalysts Supported on Alumina Spheres for Hydrogen Peroxide Decomposition," 43rd AIAA/ASME/SAE/ASEE Joint Propulsion Conference AIAA Paper 2007-5466, Cincinnati, OH, July 2007.
- [10] Russo Sorge, A., Turco, M., Pilone, G., and Bagnasco, G., "Decomposition of Hydrogen Peroxide on MnO₂/TiO₂ Catalysts," *Journal of Propulsion and Power*, Vol. 20, No. 6, 2004, p. 1069.
doi:10.2514/1.2490
- [11] Pirault-Roy, L., Kappenstein, C., Guérin, M., Eloirdi, R., and Pillet, N., "Hydrogen Peroxide Decomposition on Various Supported Catalysts Effect of Stabilizers," *Journal of Propulsion and Power*, Vol. 18, No. 6, 2002, p. 1235.
doi:10.2514/2.6058
- [12] Sahara, H., Nakasuka, S., Sugawara, Y., and Kobayashi, C., "Demonstration of Propulsion System for Microsatellite Based on Hydrogen Peroxide in SOHLA-2 Project," 43rd AIAA/ASME/SAE/ASEE Joint Propulsion Conference, AIAA Paper 2007-5575, Cincinnati, OH, July 2007.
- [13] Pasini, A., Torre, L., Romeo, L., Cervone, A., and d'Agostino, L., "Testing and Characterization of a Hydrogen Peroxide Monopropellant Thruster," *Journal of Propulsion and Power*, Vol. 24, No. 3, May-June 2008, pp. 507–515.
doi:10.2514/1.33121
- [14] Romeo, L., Pasini, A., Torre, L., d'Agostino, L., and Calderazzo, F., "Comparative Characterization of Advanced Catalytic Beds for Hydrogen Peroxide Thrusters," 44th AIAA/ASME/SAE/ASEE Joint Propulsion Conference and Exhibit, AIAA Paper 2008-5027, Hartford, CT, July 2008.
- [15] Cervone, A., Bramanti, C., d'Agostino, L., Musker, A. J., Roberts, G. T., and Saccoccia, G., "Development of Hydrogen Peroxide Monopropellant Rockets," 42nd AIAA/ASME/SAE/ASEE Joint Propulsion Conference, AIAA Paper 06-5239, Sacramento, CA, July 2006.
- [16] Romeo, L., Torre, L., Pasini, A., d'Agostino, L., and Calderazzo, F., "Development and Testing of Pt/Al₂O₃ Catalysts for Hydrogen Peroxide Decomposition," 5th International Spacecraft Propulsion Conference, Heraklion, Crete, Greece, Paper 42222, May 2008.
- [17] Kappenstein, C., Brahmi, R., Amariei, D., Batonneau, Y., Rossignol, S., and Joulin, J. P., "Catalytic Decomposition of Energetic Compounds: Influence of Catalyst Shape and Ceramic Substrate," 42nd AIAA/ASME/SAE/ASEE Joint Propulsion Conference, AIAA Paper 06-4546, Sacramento, CA, July 2006.
- [18] Goto, D., Kagawa, H., Hattori, A., and Kenichi, K., "Monopropellant Thruster Firing Test Using KC12GA Catalyst," 3rd European Workshop on Hydrazine, Cagliari, Sardinia, Italy, ESA-SP-556, 9 June 2004.

D. Talley
Associate Editor